Volume 19
Number 1

June *2017*
(ISSN 1109-1606)

Journal of

APPLIED ELECTROMAGNETISM

JAE

Trans Black Sea Region Union of Applied Electromagnetism
BSUAE

Institute of Communication and Computer Systems

Athens - GREECE

Volume 19 **June 2017**
Number 1 **(ISSN 1109-1606)**

JOURNAL
OF
APPLIED ELECTROMAGNETISM

Institute of Communication and Computer Systems

Athens - GREECE

Volume 19 **Number 1**

June 2017

TRANS BLACK SEA REGION UNION OF APPLIED ELECTROMAGNETISM (BSUAE)

JOURNAL OF APPLIED ELECTROMAGNETISM

Institute of Communication and Computer Systems

Athens - GREECE

Publishing Department

Journal of Applied Electromagnetism

Copyright Form

The undersigned I confirm that I agree the publication of the article

in the Journal of Applied Electromagnetism and the copyright to belong to Trans Black Sea Union of Applied Electromagnetism. I understand that I have the full right to reuse this manuscript for my own purposes.

Name:

Surname:

Address:

E-mail:

Signed:

***Please send the previous form signed either by e-mail to pfrangos@central.ntua.gr , or by fax to the fax number: +30 210 772 2281, attention of Prof. P. Frangos.**

Address

Institute of Communication and Computer Systems,

National Technical University of Athens,

9, Iroon Polytechniou Str.,

157 73 Athens - GREECE

Tel: (+30) 210 772 3694

Fax: (+30) 210 772 2281, attention of Prof. P. Frangos

e-mail: pfrangos@central.ntua.gr

Web site: **http://jae.ece.ntua.gr**

TRANS BLACK SEA REGION UNION OF APPLIED ELECTROMAGNETISM (BSUAE)

JOURNAL OF APPLIED ELECTROMAGNETISM (JAE)

Volume 19 Number 1 June 2017

CONTENTS

focuses on the numerical handling of a pertinent Neumann boundary value problem in the three-dimensional space acting as a tri-scale reaction – diffusion model of primary glioma growth and invasion into the surrounding normal brain. A complex anatomical and geometrical domain bounded by the skull is considered. The model takes into account the highly inhomogeneous nature of human brain. The generic finite difference – time domain (FDTD) method and more specifically the Crank – Nicolson technique in conjunction with the biconjugate gradient system solver have been utilized for the numerical solution of the problem. The model has been partly validated through comparing its predictions with real values of clinically pertinent macroscopic tumour characteristics. Numerical results are presented. They illustrate the potential of the model to support the clinician in designing the optimal individualized treatment scheme and/or schedule by using the patient's personal multiscale data and by experimenting in silico (=on the computer).

In this paper the results of a recently introduced novel solution to the well-known 'Sommerfeld radiation problem', are compared to those obtained through the classical Sommerfeld formulation. The method is novel in that it is entirely performed in the frequency domain, yielding simple integral expressions for the received Electromagnetic (EM) field and also in that they can end up into closed-form analytic formulas applicable to high frequencies. In this paper we compare our analytical results with existing numerical calculations found in the literature, based on the Sommerfeld formulation. The above comparison shows good agreement in the corresponding numerical results. Furthermore, a comparison of the method to the well-known Okumura-Hata empirical model is performed in an attempt to roughly estimate the extent to which the proposed model is suitable for real–environment EM field calculations.

EXACT MODEL MATCHING BY DYNAMIC MEASUREMENT OUTPUT FEEDBACK FOR LINEAR TIME-INVARIANT SYSTEMS

K. Kiritsis, A. Zagorianos

Hellenic Air Force Academy, Department of Aeronautical Sciences, Division of Automatic Control, Air Base of Dekelia, ΤΓΑ 1010, Dekelia, Athens, Greece.

E-mail: konstantinos.kyritsis@hafa.haf.gr

Abstract

In this paper the problem of exact model matching by dynamic measurement output feedback for linear time-invariant systems is studied. Explicit necessary and sufficient conditions are given for the problem to have a solution over the Euclidean ring of proper rational functions. A simple procedure is given for the computation of the controller that solves the problem. The design procedure consists of solving a linear equation in proper rational matrices over the Euclidean ring of proper rational functions.

1. INTRODUCTION

The exact model matching with stability by dynamic measurement output feedback was studied in [1] and [2] where necessary and sufficient conditions have been established for the existence of solution. In [3] a sufficient condition has been established for the solution of exact model matching problem with stability and an efficient computational method to determine it is given. In [4] it is studied and completely solved the exact model matching problem with stability by constant measurement output feedback for a class of linear time-invariant systems. In particular, necessary and sufficient conditions are established for the existence of solution and an algorithm to determine it is given. The purpose of this paper is to present a simple solution of the exact model matching problem by dynamic measurement output feedback for linear time-invariant systems over the Euclidean ring of proper rational functions. In particular, necessary and sufficient conditions are established which guarantee the existence of solution over the Euclidean ring of proper rational functions and a procedure is given for the computation of this solution. Our approach has certain advances over the known

results in literature [1], [2] and [3], since it proves that the existence of solution of the exact model matching problem by dynamic measurement output feedback for linear time-invariant systems over the Euclidean ring of proper rational functions depends on the infinite zero structure of proper rational matrices of mathematical model of open-loop system. The above clearly demonstrates the contribution of this paper with respect to existing results.

2. PROBLEM STATEMENT

Let us consider a linear time-invariant system with external model described by the following equations

$$\begin{bmatrix} \mathbf{y}_c(z) \\ \mathbf{y_m}(z) \end{bmatrix} = \begin{bmatrix} \mathbf{A}(z) & \mathbf{B}(z) \\ \mathbf{C}(z) & \mathbf{D}(z) \end{bmatrix} \begin{bmatrix} \mathbf{u}(z) \\ \mathbf{w}(z) \end{bmatrix} \tag{1}$$

where $\mathbf{u}(z) \in \mathbf{R}^m$ is the vector of control inputs $\mathbf{w}(z) \in \mathbf{R}^q$ is the vector of disturbance inputs, $\mathbf{y}_m(z) \in \mathbf{R}^p$ is the available measurement output vector, $\mathbf{y}_c(z) \in \mathbf{R}^s$ is the vector of outputs to be controlled and $\mathbf{A}(z)$, $\mathbf{B}(z)$, $\mathbf{C}(z)$ and $\mathbf{D}(z)$ are proper rational matrices of appropriate dimensions. The exact model matching problem by dynamic measurement output feedback is defined as follows. Find the controller:

$$\mathbf{u}(z) = \mathbf{F}(z)\mathbf{y}_m(z) \tag{2}$$

where $\mathbf{F}(z)$ is proper rational matrix of appropriate dimensions, so that the transfer function $\mathbf{T}_c(z)$ relating $\mathbf{w}(z)$ and $\mathbf{y}_c(z)$ of the compensated system:

$$\mathbf{T}_c(z) = \mathbf{A}(z)\mathbf{F}(z)[\mathbf{I} - \mathbf{C}(z)\mathbf{F}(z)]^{-1}\mathbf{D}(z) + \mathbf{B}(z) \tag{3}$$

is a prescribed proper and stable rational matrix $\mathbf{H}(z)$. In particular, we will examine if there exists a dynamic output feedback (2) such that

$$\mathbf{T}_c(z) = \mathbf{H}(z) \tag{4}$$

If so, give necessary and sufficient conditions for existence and a procedure to calculate $\mathbf{F}(z)$.

3. BASIC CONCEPTS AND PRELIMINARY RESULTS

Let $\mathbf{R}_{\mathrm{p}}(\mathrm{z})$ be the Euclidean ring of proper rational functions in z. A matrix $\mathbf{W}(\mathrm{z})$ whose elements are proper rational functions is called proper rational matrix. A square matrix $\mathbf{U}(\mathrm{z})$ over $\mathbf{R}_{\mathrm{p}}(\mathrm{z})$ is said to be biproper if its inverse exists and is also proper. A conceptual tool for the study of the structure of rational matrices is the following standard form. Every proper rational matrix $\mathbf{W}(\mathrm{z})$ of dimensions *p x m* with rank$\mathbf{W}(\mathrm{z})= r$, can be expressed as:

$$\mathbf{W}(\mathrm{z}) = \mathbf{U}_1(\mathrm{z})\, \mathbf{M}(\mathrm{z})\, \mathbf{U}_2(\mathrm{z}) \tag{5}$$

The matrices $\mathbf{U}_1(\mathrm{z})$ and $\mathbf{U}_2(\mathrm{z})$ are biproper and the matrix $\mathbf{M}(\mathrm{z})$ is given by:

$$\mathbf{M}(\mathrm{z}) = \begin{bmatrix} \mathbf{M}_r(\mathrm{z}) & \mathbf{0} \\ \mathbf{0} & \mathbf{0} \end{bmatrix} \tag{6}$$

where $\mathbf{M}_r(\mathrm{z}) = \mathrm{diag}\left[\mathrm{z}^{-\delta 1}, \ldots\ldots, \mathrm{z}^{-\delta \mathrm{r}}\right]$ and $\delta_1 \leq \ldots \leq \delta_r$ are nonnegative integers uniquely determined by $\mathbf{W}(\mathrm{z})$. This is the Smith-McMillan form over $\mathbf{R}_{\mathrm{p}}(\mathrm{z})$ [5], [6] and the non-negative integers δ_i for *i =1, 2, ...,.r*, determine the structure of the infinite zero of $\mathbf{W}(\mathrm{z})$.

The following Lemmas are taken from [5] and are needed to prove the main theorem of this paper.

Lemma 1. Let $\mathbf{P}(\mathrm{z})$ and $\mathbf{Q}(\mathrm{z})$ be rational matrices with elements in $\mathbf{R}_{\mathrm{p}}(\mathrm{z})$. Then the equation:

$$\mathbf{P}(\mathrm{z})\mathbf{X}(\mathrm{z}) = \mathbf{Q}(\mathrm{z}) \tag{7}$$

has a solution over $\mathbf{R}_{\mathrm{p}}(\mathrm{z})$ if and only if the matrices $\mathbf{P}(\mathrm{z})$ and $[\mathbf{P}(\mathrm{z}), \mathbf{Q}(\mathrm{z})]$ have the same infinite zero structure.

Lemma 2. Let $\mathbf{N}(\mathrm{z})$ and $\mathbf{R}(\mathrm{z})$ be rational matrices with elements in $\mathbf{R}_{\mathrm{p}}(\mathrm{z})$. Then the equation:

$$\mathbf{Y}(\mathrm{z})\mathbf{N}(\mathrm{z}) = \mathbf{R}(\mathrm{z}) \tag{8}$$

has a solution over $\mathbf{R}_{\mathrm{p}}(\mathrm{z})$ if and only if the matrices $\mathbf{N}(\mathrm{z})$ and $\begin{bmatrix}\mathbf{N}(\mathrm{z})\\ \mathbf{R}(\mathrm{z})\end{bmatrix}$ have the same infinite zero structure.

4. MAIN RESULTS

Let rank$[\mathbf{A}(\mathrm{z})]=r$ then there exists biproper matrices $\mathbf{U}_1(\mathrm{z})$ and $\mathbf{U}_2(\mathrm{z})$ [6] which reduce $\mathbf{A}(\mathrm{z})$ to the Smith–McMillan form over $\mathbf{R}_{\mathrm{p}}(\mathrm{z})$:

$$\mathbf{A}(\mathrm{z}) = \mathbf{U}_1(\mathrm{z}) \begin{bmatrix}\mathbf{A}_r(\mathrm{z}) & \mathbf{0}\\ \mathbf{0} & \mathbf{0}\end{bmatrix} \mathbf{U}_2(\mathrm{z}) \tag{9}$$

where $\mathbf{A}_r(\mathrm{z}) = \mathrm{diag}\left[\mathrm{z}^{-\delta 1}, \ldots\ldots, \mathrm{z}^{-\delta r}\right]$. The non-negative integers δ_i for *i =1, 2, ….,r*, determine the structure of the infinite zero of $\mathbf{A}(\mathrm{z})$. Let also:

$$\mathbf{L}(\mathrm{z}) = \mathbf{H}(\mathrm{z}) - \mathbf{B}(\mathrm{z}) \tag{10}$$

Denote

$$\mathbf{U}_1^{-1}(\mathrm{z})\, \mathbf{L}(\mathrm{z}) = \begin{bmatrix}\mathbf{L}_1(\mathrm{z})\\ \mathbf{L}_2(\mathrm{z})\end{bmatrix} \tag{11}$$

The matrix $\mathbf{L}_1(\mathrm{z})$ in (11) has *r* rows.

The main result of this paper is given below, in particular the main theorem of this section gives necessary and sufficient conditions for the existence of a dynamic measurement output feedback that solves the exact model matching problem over the Euclidean ring of proper rational functions.

Theorem. The exact model matching problem by dynamic measurement output feedback has a solution over $\mathbf{R}_{\mathrm{p}}(\mathrm{z})$ if and only if the following conditions hold:

(a) The matrices $\mathbf{A}(\mathrm{z})$ and $[\mathbf{A}(\mathrm{z}), \mathbf{L}(\mathrm{z})]$ have the same infinite zero structure.

(b) The matrices $\mathbf{D}(\mathrm{z})$ and $\begin{bmatrix}\mathbf{D}(\mathrm{z})\\ \mathbf{A}_r^{-1}(\mathrm{z})\mathbf{L}_1(\mathrm{z})\end{bmatrix}$ have the same infinite zero structure.

Proof: To prove necessity, write the transfer function of the closed – loop system given by equation (3) as follows:

$$\mathbf{T}_{\mathrm{c}}(\mathrm{z}) = \mathbf{A}(\mathrm{z})\mathbf{X}(\mathrm{z})\, \mathbf{D}(\mathrm{z}) + \mathbf{B}(\mathrm{z}) \tag{12}$$

where the matrix $\mathbf{X}(z)$ is given by:

$$\mathbf{X}(z) = \mathbf{F}(z)[\mathbf{I} - \mathbf{C}(z)\mathbf{F}(z)]^{-1} \tag{13}$$

Suppose that the exact model matching problem by dynamic measurement output feedback has a solution. Then equation (12) can be rewritten as follows:

$$\mathbf{A}(z)\mathbf{X}(z)\mathbf{D}(z) + \mathbf{B}(z) = \mathbf{H}(z) \tag{14}$$

Using equation (10), equation (14) can be rewritten as follows:

$$\mathbf{A}(z)\mathbf{X}(z)\mathbf{D}(z) = \mathbf{H}(z) - \mathbf{B}(z) = \mathbf{L}(z) \tag{15}$$

If we define $\mathbf{Y}(z) = \mathbf{X}(z)\mathbf{D}(z)$ then equation (15) can be rewritten as follows:

$$\mathbf{A}(z)\mathbf{Y}(z) = \mathbf{L}(z) \tag{16}$$

Since by assumption the exact model matching problem by dynamic measurement output feedback has a solution, the equation (15) has a solution for $\mathbf{X}(z)$ over $\mathbf{R}_p(z)$ and therefore equation (16) has also a solution for $\mathbf{Y}(z)$ over $\mathbf{R}_p(z)$. Hence, according to Lemma 1 the matrices $\mathbf{A}(z)$ and $[\mathbf{A}(z), \mathbf{L}(z)]$ have the same infinite zero structure. This is the condition (a) of the Theorem. Using (9) equation (15) can be rewritten as follows:

$$\mathbf{U}_1(z)\begin{bmatrix}\mathbf{A}_r(z) & \mathbf{0}\\ \mathbf{0} & \mathbf{0}\end{bmatrix}\mathbf{U}_2(z)\,\mathbf{X}(z)\,\mathbf{D}(z) = \mathbf{L}(z) \tag{17}$$

Or equivalently:

$$\begin{bmatrix}\mathbf{A}_r(z) & \mathbf{0}\\ \mathbf{0} & \mathbf{0}\end{bmatrix}\mathbf{U}_2(z)\,\mathbf{X}(z)\,\mathbf{D}(z) = \mathbf{U}_1^{-1}(z)\,\mathbf{L}(z) \tag{18}$$

Using equation (11), equation (18) can be rewritten as follows:

$$\begin{bmatrix}\mathbf{A}_r(z) & \mathbf{0}\\ \mathbf{0} & \mathbf{0}\end{bmatrix}\mathbf{U}_2(z)\,\mathbf{X}(z)\,\mathbf{D}(z) = \begin{bmatrix}\mathbf{L}_1(z)\\ \mathbf{L}_2(z)\end{bmatrix} \tag{19}$$

From equation (19) we have that:

$$[\,\mathbf{A}_r(\mathrm{z})\ \mathbf{0}]\mathbf{U}_2(\mathrm{z})\,\mathbf{X}(\mathrm{z})\,\mathbf{D}(\mathrm{z}) = \mathbf{L}_1(\mathrm{z}) \tag{20}$$

Or equivalently:

$$\mathbf{\Phi}(\mathrm{z})\,\mathbf{D}(\mathrm{z}) = \mathbf{A}_r^{-1}(\mathrm{z})\mathbf{L}_1(\mathrm{z}) \tag{21}$$

Where the matrix $\mathbf{\Phi}(\mathrm{z})$ over $\mathbf{R}_{\mathrm{p}}(\mathrm{z})$ is given by:

$$\mathbf{\Phi}(\mathrm{z}) = [\mathbf{I}_r \quad \mathbf{0}]\,\mathbf{U}_2(\mathrm{z})\,\mathbf{X}(\mathrm{z}) \tag{22}$$

Since by assumption $\mathbf{X}(\mathrm{z})$ exists and is proper as well, equation (21) has a solution for $\mathbf{\Phi}(\mathrm{z})$ over $\mathbf{R}_{\mathrm{p}}(\mathrm{z})$. Hence according to lemma 2 the matrices $\mathbf{D}(\mathrm{z})$ and $\begin{bmatrix}\mathbf{D}(\mathrm{z})\\ \mathbf{A}_r^{-1}(\mathrm{z})\mathbf{L}_1(\mathrm{z})\end{bmatrix}$ have the same infinite zero structure. This is the condition (b) of the Theorem.

The sufficiency of conditions (a) and (b) can be proved as follows. Condition (a) guarantees that the matrix $\mathbf{L}_2(\mathrm{z})$ in (19) is zero. Since $\mathbf{L}_2(\mathrm{z}) = \mathbf{0}$ and the rational matrix $\mathbf{A}_r(\mathrm{z})$ is nonsingular, equation (15) is equivalent to equation (21). Then according to Lemma 2, condition (b) guarantees that the equation (21) has a solution for $\mathbf{\Phi}(\mathrm{z})$ over $\mathbf{R}_{\mathrm{p}}(\mathrm{z})$. Since $\mathbf{\Phi}(\mathrm{z})$ is a solution over $\mathbf{R}_{\mathrm{p}}(\mathrm{z})$ of equation (21), from relationship (22) it follows that:

$$\mathbf{X}(\mathrm{z}) = \mathbf{U}_2^{-1}(\mathrm{z})\begin{bmatrix}\mathbf{\Phi}(\mathrm{z})\\ \mathbf{0}\end{bmatrix} \tag{23}$$

is a solution over $\mathbf{R}_{\mathrm{p}}(\mathrm{z})$ of equation (15) or equivalently of equation (12). Furthermore from (13) it follows that:

$$\mathbf{F}(\mathrm{z}) = [\mathbf{X}(\mathrm{z})\mathbf{C}(\mathrm{z}) + \mathbf{I}]^{-1}\mathbf{X}(\mathrm{z}) \tag{24}$$

The matrix $\mathbf{F}(\mathrm{z})$ given by (24) with $\mathbf{X}(\mathrm{z})$ given by (23) is proper and satisfies equation (3) and therefore the exact model matching problem by dynamic measurement output feedback has a solution over $\mathbf{R}_{\mathrm{p}}(\mathrm{z})$. This completes the proof.

5. COMPUTATION OF THE CONTROLLER

In this section a procedure is given for the calculation of proper solution of exact model matching problem by dynamic measurement output feedback.

Given: $\mathbf{A}(z), \mathbf{B}(z), \mathbf{C}(z), \mathbf{D}(z)$ and $\mathbf{H}(z)$

Find: $\mathbf{F}(z)$

Step 1. Let rank $\mathbf{A}(z) = r$. Find biproper matrices $\mathbf{U}_1(z)$ and $\mathbf{U}_2(z)$ [6], which reduce $\mathbf{A}(z)$ to the Smith–McMillan form over $\mathbf{R}_p(z)$.

$$\mathbf{A}(z) = \mathbf{U}_1(z) \begin{bmatrix} \mathbf{A}_r(z) & \mathbf{0} \\ \mathbf{0} & \mathbf{0} \end{bmatrix} \mathbf{U}_2(z)$$

where $\mathbf{A}_r(z) = \text{diag}\left[z^{-\delta 1}, \ldots\ldots, z^{-\delta r}\right]$. Let $\mathbf{L}(z)=\mathbf{H}(z)-\mathbf{B}(z)$. Denote

$$\mathbf{U}_1^{-1}(z)\, L(z) = \begin{bmatrix} \mathbf{L}_1(z) \\ \mathbf{L}_2(z) \end{bmatrix}$$

where $\mathbf{L}_1(z)$ has *r* rows.

Step 2. Check the conditions (a) and (b) of the Theorem. If these conditions are satisfied go to step 3. If not go to step 6.

Step 3. Solve equation (21) and find $\mathbf{\Phi}(z)$.

Step 4. Set

$$\mathbf{X}(z) = \mathbf{U}_2^{-1}(z) \begin{bmatrix} \mathbf{\Phi}(z) \\ \mathbf{0} \end{bmatrix}$$

Step 5. Set

$$\mathbf{F}(z) = [\mathbf{X}(z)\mathbf{C}(z) + \mathbf{I}]^{-1}\mathbf{X}(z)$$

Step 6. Our problem has no solution.

6. CONCLUSIONS

In this paper the solution of exact model matching problem by dynamic measurement output feedback over the Euclidean ring of proper rational functions is studied. Necessary and sufficient conditions have been established for the problem to

have a solution. A simple procedure is given for the computation of the dynamic controller that solves the problem. The design procedure consists of solving a linear equation in proper rational matrices over the Euclidean ring of proper rational functions. In our point of view the main results of this paper are useful for further understanding of exact model matching problem with stability by dynamic measurement output feedback.

REFERENCES

[1] D.Y. Ohm, J.W. Howze and S.P. Bhattacharrya,"Structural synthesis of multivariable Controllers", Automatica, Vol.21, No.1, pp.35-55, 1985.

[2] A. B. Ozguler and V. Eldem, "Disturbance decoupling via dynamic output feedback", IEEE Transactions on Automatic Control, Vol.30, No.8, pp.756-764, 1985.

[3] Z. Gao and P. J. Antsaklis., "On stable solution of one and two-sided model matching problems", IEEE Transactions on Automatic Control, Vol.34, No.9, pp.978 - 982, 1989.

[4] T.G. Koussiouris, K.H. Kiritsis, "Two-sided model matching by measurement output feedback for linear time-invariant systems", Proceedings of the 2nd International Conference on Circuits, Systems and Computers, pp.374-377, 1998.

[5] V. Kucera, "Analysis and Design of Discrete Linear Control Systems", Prentice Hall, pp.24-28, 1991.

[6] A.I.G. Vardulakis, D.N. Limebeer and N. Karcanias, "Structure and Smith–McMillan form of a rational matrix at infintity", International Journal of Control, Vol. 35, No. 4 pp. 701-725, 1982.

HUMAN EXPOSURE STUDY FOR SOME SCENARIOS (selected from CEMA'16 Conference)

T. Nozadze, R. Zaridze, V. Jeladze, V. Tabatadze, I. Petoev, M. Prishvin

Tbilisi State University, Laboratory of Applied Electrodynamics and Radio Engineering

3, Chavchavadze Ave. Tbilisi, Georgia

Email : tamar.nozadze002@ens.tsu.edu.ge, revaz_zaridze@mail.ru, veriko.jeladze001@ens.tsu.edu.ge

Abstract

In this article the main aim of the research is to investigate EM exposure influence on a human homogenous model located in a car and study possible resonant fields. This problem is very topical, because in some cases the excitation source is located in vicinity to the sensitive tissues. We have investigated several cases when a human with a cellphone is located inside a car and also the case when the EM source is the base station antenna. The problems are solved using the Method of Auxiliary Sources (MAS) with a user friendly program package, created for numerical experiments realization for these particular problems. The results of the numerical experiment are presented and analyzed.

1. INTRODUCTION

With the rapid development of new technologies, such as mobile phones and other communication systems, exposure of users to electromagnetic fields (EMF) has enormously increased in recent years. It is important to study their EM influence on human, because excitation source is located very close to the sensitive tissue. Also it is important to obtain some general conclusions about the nature of exposure process, in order to elaborate some safety recommendations and standards. Our goal in this research is to investigate EM influence on human, when it is located inside the car and study the fields' behavior in the near and far zone. There are many factors to consider, like complex body geometry [1], [2], location in an enclosed or semi-enclosed room, wall transparency and users hand position, etc. It is impossible to thoroughly quantitatively consider all these details, but we can estimate most importance of them.

In spite of many works on this issue, the problem is not studied completely. EM absorption by human is measured in terms of specific absorption rate (SAR) [3] and it is measured in watt per kilogram (W/kg) [4]. In the article [5] are investigated several scenarios with Mummy: one is when the Mummy is located inside of a room while talking over the mobile phone. The other is when the Mummy is located inside of the room but the EM source is a base station antenna located outside. For these cases are studied the influence of the room walls transparency on the formation of the near field inside the room and far field pattern. As the numerical experiments shows, in some cases, the room behaves as a resonator and amplifies the radiated field. The field value may be amplified and be dangerous for the user. The Method of Auxiliary Sources is used to solve efficiently all these problems [6].

2. MODELS, METHODS AND RESULTS OF NUMERICAL SIMULATIONS

During the EM Exposure influence investigation, it is forbidden to conduct real experiments on humans. Because of this the main tools of investigation represents the computer modeling based on numerical methods. There are studied two cases: first when EM source is inside the car and second case when EM source is base station antenna located outside, for both cases human is located inside the car. We use a homogenous dielectric human shaped body 'Mummy' with averaged permittivity and losses values (according to muscle, bone and blood), since their inhomogeneity does not affect the final results significantly. The use of such model is needed to implement the Method of Auxiliary Sources for calculations diffraction problems on human model for the big scenarios, when it is located inside the car. It is important to take into account the possible resonant effects in the car, study SAR distributions for the human model and near and far field distribution in case of mobile phone and base station antenna.

Application of the MAS is deduced to the construction of two couples of closed auxiliary surfaces inside and outside of the "Mummy" and also inside and outside of the surrounded semi open surface like the car (figure 1). Along the surfaces of the "Mummy" and so called the car, as it is possible homogeneously, we distribute the N and M numbers of points, correspondingly. On these auxiliary surfaces from both sides are distributed the same numbers combined auxiliary sources with unknown complex coefficients, which

have meaning of the criterion weigh. These unknown complex amplitudes of the auxiliary sources must be found by the boundary conditions satisfaction using the collocation method for the scattered field on the human body model - as on the dielectric (the continuity of the electric and magnetic field tangential components). On the semi open surface inside and outside (the tangential component of the electric field must be zero) and on the open parts (windows) of the car (as on the dielectric) – continuity of the fields.

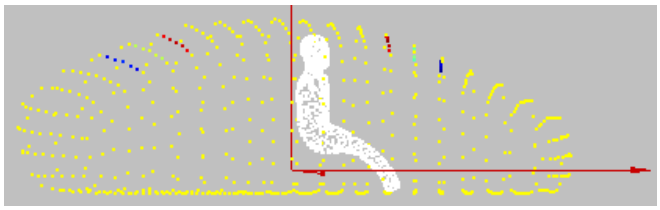

Figure 1. MAS model of cavity with using auxiliary surfaces.

The calculations were conducted at the 300 MHZ and 450 MHZ frequencies. The combined dipole (Huygens source) was used as auxiliary source for the calculations.

In this paper we introduce a new approach to use the MAS methodology. Our final goal is to find the near field distribution inside of the human body as well as inside and outside of the car. We consider human homogenous model like Mummy, with complex permittivity, $\varepsilon=45+i2$, (an averaged value considering blood, muscle and bones). Several scenarios have been studied (when source is mobile phone and base station antenna). The EM field incidence angle is 30^0 which means, that base station antenna is located sufficiently near. Obtained results are presented below. Values of the near field distribution and SAR are provided in the relative units.

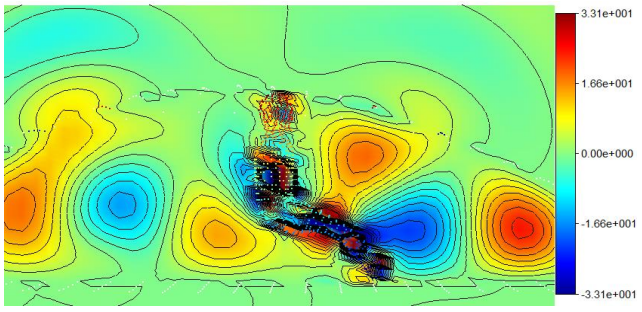

a)

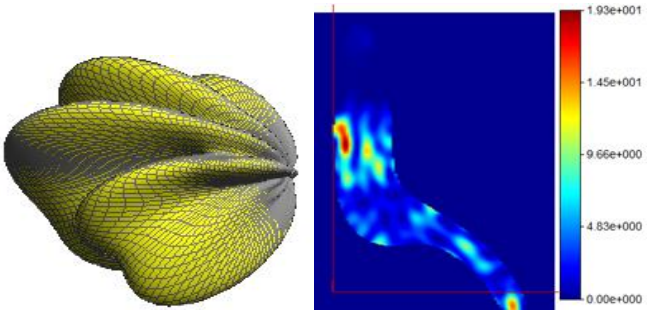

b) c)

Figure 2. Near field distribution in the car (a) and far field pattern (b), SAR distribution inside of human body (c) at 300 MHz (source is inside the car).

In the fig.2 a) and fig.3 a) are presented near field distribution in the car, far field pattern and SAR distribution inside of the head at the 300 MHz and 450 MHz, when source is mobile phone are shown on fig.2 b), fig.3 b) and fig.2 c) and fig.3 c) respectively. As it seen from the obtained results at the 300 MHz inside the car is created high reactive field, which might be dangerous for human.

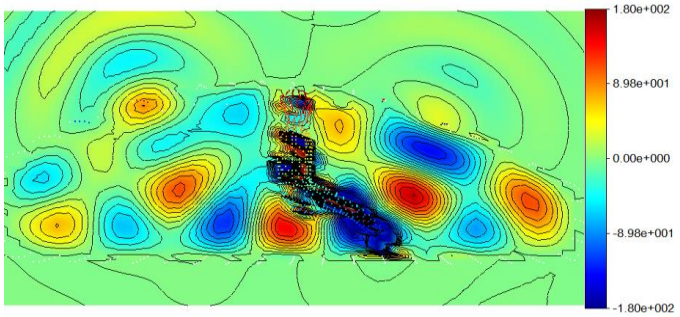

a)

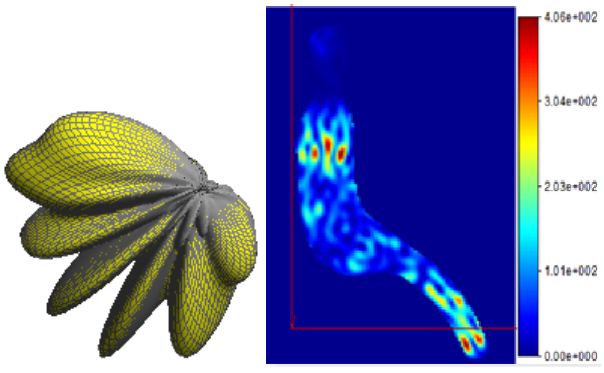

b) c)

Figure 3. Near field distribution in the car (a) and far field pattern (b), SAR distribution inside of human body (c) at 450 MHz (source is inside the car).

The results show that the resonant field is generated inside the car for both 300 MHz and 450 MHz frequencies, the part of radiated energy is goes through the window and the significant part is absorbed by the human body. At 450 MHz frequency the field value about six times higher than for 300 MHz frequency. As we see from these results at the 450 MHz pick SAR value one order higher than at the 300 MHz frequency.

The near field distribution for the case when the source is the base station antenna is shown of fig.4 a). The far field pattern and SAR distribution inside of human head at the 450 MHz are presented on fig. 4 b) and c) respectively.

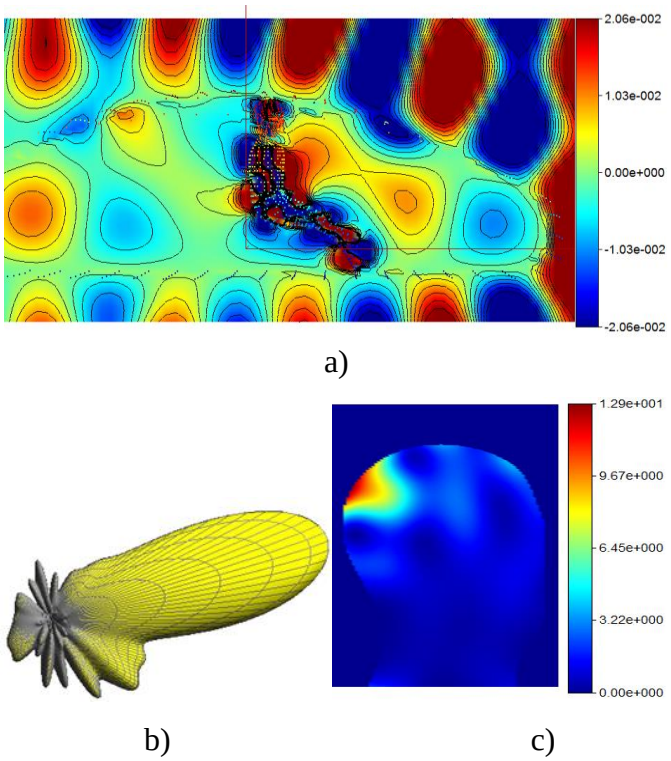

Figure 4. Near field distribution in the car (a) and far field pattern (b), SAR distribution inside of human head (c) at 300 MHz (source is base station antenna).

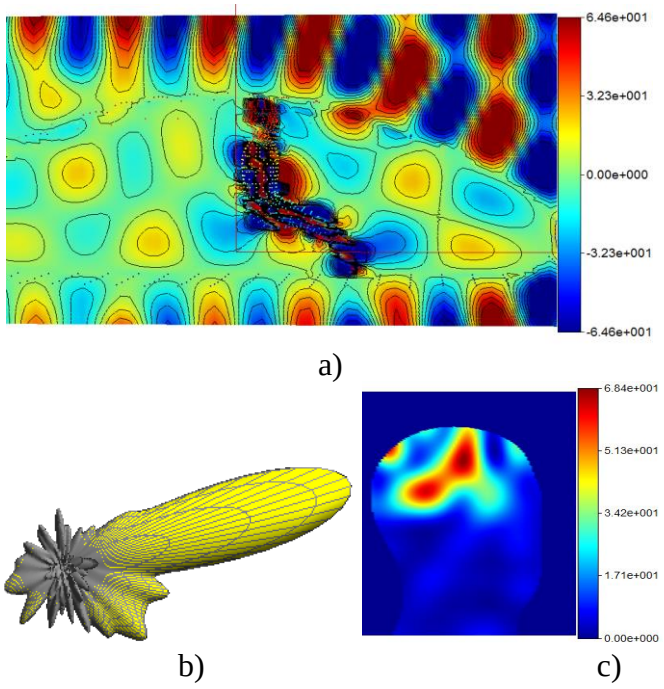

Figure 5. Near field distribution in the car (a) and far field pattern (b), SAR distribution inside of human head (c) at 450 MHz (source is base station antenna).

At the 450 MHz frequency, in case when source is base station antenna, obtained results are presented on the fig.5. The near field distribution for this case is shown on fig.5 a). For far field pattern we got result which is presented on fig.5 b) and SAR distribution inside of human head is shown on fig.5 c).

The EM field reaches inside the car through the window and the most part of this field energy is absorbed by the human body. For both cases the field values are smaller than in case when the EM source is inside the car, because the source is far from the human body. The obtained results show, that in case when EM source is base station antenna, pick SAR value at the 450 MHz is about five times higher than at the 300 MHz frequency. If we compare the obtained results all these considered cases, we see that reactive field and pick SAR values are higher in case when EM source is inside the car.

3. CONCLUSION

In this research we introduce a new approach to use the MAS methodology. There was considering human homogenous model like Mummy. We study far field pattern and near field distribution inside of the human body as well as inside and outside

of the car. Also we study SAR distribution inside the homogenous human model head and we see that reactive field and pick SAR values are higher in case when EM source is inside the car, then in case when source is base station antenna.

Based on the obtained results we can make the following safety recommendation: It is not desirable speak on phone for a long time if user is located inside the car. The calculations, conducted with the created program package, showed the presence of resonance and reactive fields in several big scenarios, which could be dangerous for a human. It is important to note, that we study electromagnetic exposure problem for one human model, in some cases the results will not be applicable for other models. Every human is unique and differs in form, dimensions, weight and so more studies may be needed to make a firm conclusion.

ACKNOWLEDGEMENT

This study is supported by Shota Rustaveli National Science Foundation grant: YS15_2.12_56.

REFERENCES

[1] J. Krogerus, J. Toivanen, C. Icheln, and P. Vainikainen, “Effect of the human body on total radiated power and the 3-d radiation pattern of mobile handsets,” IEEE Trans. Instrum. Meas., vol. 56, no. 6, Dec. 2007, pp. 2375–2385

[2] M. R. I. Faruque, M. T. Islam, N. Misran, “Effect of human head shapes for mobile phone exposure on electromagnetic absorption”, Informacije MIDEM- Journal of Microelectronics, Electronic Components and Materials, vol. 40, no. 3, 2010, pp. 232-23

[3] A. H. Kusuma et al., “A new low SAR antenna structure for wireless handset applications”, Progress in Electromagnetics Research, vol. 112, pp. 23-40, 2011.

[4] M. R. I. Faruque et al., “Effect of human head shapes for mobile phone exposure on electromagnetic absorption”, Informacije MIDEM, vol. 40, no. 3, pp. 232- 237, 2010.

[5] V. Jeladze, I. Petoev, V. Tabatadze, M. Prishvin, R. Zaridze, "The Method of Auxiliary Sources for Study of Resonant Field Effects upon a Human Models for Big Scenarios", Journal of Communications Technology and Electronics, Moscow, Russia.

[6] J. A. Stratton. Theory of Electromagnetism. Moscow: OGIZ, 1948, pp. 383-387.

IN SILICO SIMULATION OF GLIOBLASTOMA GROWTH AND INVASION INTO THE HUMAN BRAIN INCLUDING AN EXPLICIT MODELLING OF THE ADIABATIC BOUNDARY CONDITION IMPOSED BY THE SKULL

(selected from CEMA'16 Conference)

S. Giatili, G. Stamatakos

Institute of Communication and Computer Systems,
School of Electrical and Computer Engineering
National Technical University of Athens,
In Silico Oncology and In Silico Medicine Group,
9 Iroon Polytechniou, GR157 80, Zografos, Greece.
Email: gestam@central.ntua.gr

Abstract

The diffusive and infiltrative nature of glioma brain tumours and in particular glioblastoma constitutes a major barrier to their effective treatment. The present paper focuses on the numerical handling of a pertinent Neumann boundary value problem in the three-dimensional space acting as a tri-scale reaction – diffusion model of primary glioma growth and invasion into the surrounding normal brain. A complex anatomical and geometrical domain bounded by the skull is considered. The model takes into account the highly inhomogeneous nature of human brain. The generic finite difference – time domain (FDTD) method and more specifically the Crank – Nicolson technique in conjunction with the biconjugate gradient system solver have been utilized for the numerical solution of the problem. The model has been partly validated through comparing its predictions with real values of clinically pertinent macroscopic tumour characteristics. Numerical results are presented. They illustrate the potential of the model to support the clinician in designing the optimal individualized treatment scheme and/or schedule by using the patient's personal multiscale data and by experimenting in silico (=on the computer).

1. INTRODUCTION

Malignant gliomas, in general, and astrocytomas, in particular, account for approximately 50% of primary central nervous system (CNS) tumours in adults [1]. The

median survival for glioblastoma multiforme (GBM) is 10-12 months. Because of the infiltrative nature of malignant gliomas [1,2], even a gross total resection is associated with tumour recurrence. In order to partly alleviate the corresponding complex treatment problem, cancer mathematical modelling [3] of diffusive tumour growth has been proposed and a number of models have been developed [2, 4]. The practical goal of this work, which can be viewed as a synthesis and an important extension of previous efforts [4], is to develop a "bottom-up" tri-scale diffusion-reaction based mathematical model of glioma growth and invasion that would serve as the core of the "Continuous Mathematics Based GBM Oncosimulator." [3]. For a biologically meaningful and computationally reliable diffusion-reaction based solution to the problem, consideration of the actual physical boundary of the cranium is important. An improper handling of the boundary conditions may lead to an unnatural behaviour of the simulated system and artificial loss of tumour cells. The model focuses primarily on the detailed numerical handling of the adiabatic Neumann boundary conditions imposed by the presence of the skull, considering the spatiotemporal characteristics of glioblastoma invasion.

2. THE TRI-SCALE REACTION – DIFFUSION MODEL

If Ω is the brain domain, GBM tumour growth and brain infiltration can be expressed by equation [5]:

$$\frac{\partial c(\vec{x},t)}{\partial t} = \nabla\cdot[D(\vec{x})\ \nabla c(\vec{x},t)] + \rho\ c(\vec{x},t) - G(t)c(\vec{x},t) \text{ in } \Omega \qquad (1)$$

where $\frac{\partial c(\vec{x},t)}{\partial t}$ denotes the rate of change of tumour cell concentration c at any spatial point $\vec{x}$ and time t, D denotes the diffusion coefficient and represents the active motility of tumour cells, $\rho\, c(\vec{x},t)$ expresses the net proliferation of tumour cells and $G(t)c(\vec{x},t)$ defines the loss of tumour cells due to treatment and also indirectly involves insufficient and inadequate angiogenesis.

The model takes into account the highly inhomogeneous nature of human brain. Two different approaches have been developed: the homogeneous and the inhomogeneous approach. In the inhomogenous approach, the structures of white matter, grey matter, cerebrospinal fluid (CSF) are taken into consideration and three values of the

parameter D are considered: D_g, D_w and D_{CSF} if $(\vec{x})$ belongs to grey matter, white matter and CSF respectively. In the homogenous approach, where for simplification homogeneous brain tissue is considered, D has the same value all over the intracranial space.

Regarding the initial condition for the reaction–diffusion system, it is assumed that the initial spatial distribution of malignant cells is described by a known function $f(\vec{x})$. In order to complete the model formulation, appropriate boundary conditions have to be added precluding migration beyond the skull boundary. Neumann boundary conditions, which correspond to no net flow of tumour cells out of or into the brain region across the brain-skull boundary, have been imposed.

In order to numerically apply the Neumann boundary condition, "fictitious nodes", $F_{i,j,k}$, have been used [6]. Their number is equal to the number of the adjacent nodes that belong to the cranium. An indicative case of numerically applying the boundary condition at the boundary point (x_i, y_j, z_k) in the negative z direction is the following:

$$-\left.\frac{\partial c}{\partial z}\right|_{(x_i,y_j,z_k)} = 0 \Rightarrow c_{i,j,k+1} = c_{F_{i,j,k-1}} \tag{2}$$

An indicative equation at the boundary grid point (x_i , y_j, z_k) where skull tissue is found only in the negative x and the negative y direction by applying the Crank - Nicolson scheme is (3) for the homogeneous and (4) for the inhomogeneous approach respectively.

$$[1+6\lambda-\frac{\Delta t}{2}(\rho-G)]c_{i,j,k}^{t+1}-\lambda(2c_{i+1,j,k}^{t+1}+2c_{i,j+1,k}^{t+1}+c_{i,j,k+1}^{t+1}+c_{i,j,k-1}^{t+1})=$$
$$[1-6\lambda+\tfrac{\Delta t}{2}(\rho-G)]c_{i,j,k}^{t}+\lambda(2c_{i+1,j,k}^{t}+2c_{i,j+1,k}^{t}+c_{i,j,k+1}^{t}+c_{i,j,k-1}^{t}) \tag{3}$$

$$\left[1+6\lambda_{i,j,k}-\frac{\Delta t}{2}(\rho-G)\right]c_{i,j,k}^{t+1}-2\lambda_{i,j,k}c_{i+1,j,k}^{t+1}-2\lambda_{i,j,k}c_{i,j+1,k}^{t+1}-\left(\lambda_{i,j,k}+\frac{\lambda_{i,j,k+1}-\lambda_{i,j,k-1}}{4}\right)c_{i,j,k+1}^{t+1}-\left(\lambda_{i,j,k}-\frac{\lambda_{i,j,k+1}-\lambda_{i,j,k-1}}{4}\right)c_{i,j,k-1}^{t+1}=$$
$$\left[1-6\lambda_{i,j,k}+\frac{\Delta t}{2}(\rho-G)\right]c_{i,j,k}^{t}+2\lambda_{i,j,k}c_{i+1,j,k}^{t}+2\lambda_{i,j,k}c_{i,j+1,k}^{t}+\left(\lambda_{i,j,k}+\frac{\lambda_{i,j,k+1}-\lambda_{i,j,k-1}}{4}\right)c_{i,j,k+1}^{t}+\left(\lambda_{i,j,k}-\frac{\lambda_{i,j,k+1}-\lambda_{i,j,k-1}}{4}\right)c_{i,j,k-1}^{t} \tag{4}$$

where $c^{t}_{i,j,k}$ is the finite difference approximation of c at the grid point (x_i y_j, z_k) at time t, Δt is the time step size for the time discretization, h is the space step size at each axis of the gridding scheme for the space discretization, $\lambda = D\Delta t / [2(h)^2]$ and $\lambda_{i,j,k} = D_{i,j,k}\Delta t / [2(h)^2]$. The resulting system of equations may be written equivalently in the form $\overleftrightarrow{A}\,\vec{x} = \vec{b}$ where $\vec{x}$ denotes a vector that contains an approximation of the solution c at the mesh nodes at time t. Due to the high complexity of the biological system the Bi-Conjugate Gradient method (BiCG) has been applied [6].

3. MODEL SIMULATIONS

Three-dimensional simulations of untreated glioma growth, assuming a complex anatomical and also geometrical domain bounded by the skull, have been performed. A three dimensional image of a typical real human head has been considered. The dataset used has been acquired from 3d Slicer which is a freely available application for image analysis and automatic segmentation of brain structures from MRI data. Two different scenarios have been executed and mutually compared; the homogeneous and the inhomogeneous scenarios. In the first case homogeneous brain tissue is considered. In the second case the structures of white matter, grey matter, CSF and skull have been segmented. Following the delineation of the skull boundary, a fictitious growing virtual spherical glioblastoma tumour of radius equal to 0.7 cm has been virtually placed inside the cranial cavity. It should be noted that glioblastoma diagnosis is possible when the volume of an enhanced CT-detectable tumour has reached a size equivalent to a sphere with an average 3 cm diameter [5].

The typical values of the parameters that have been used for the production of the results have been carefully selected from pertinent literature so as to best reflect aspects of glioblastoma dynamics. The net tumour growth rate ρ, which represents the net rate of tumour growth including tumour cell proliferation, loss and death has been set equal to 0.012 d-1 [5]. For the inhomogeneous scenario the value of the space dependent diffusion coefficient Di,j,k, has been calculated as the average value of the growing diffusion coefficient and the migrating diffusion coefficient (Dg =0.000102cm2/d, Dw=0.00051cm2/d and DCSF=0.000001 cm2/d) [7].

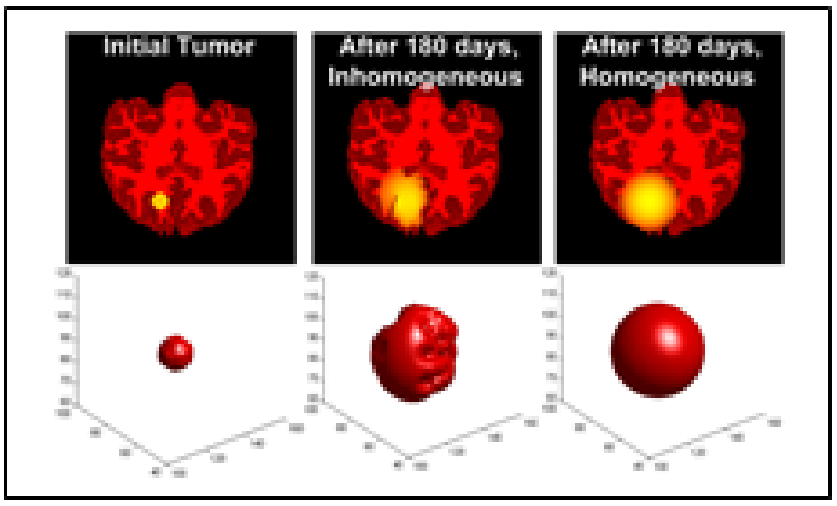

Figure 1. Coronal slice and a three dimensional snaphot of a virtual tumour for the inhomogeneous (second panel column) and homogeneous (third panel column) case after 180 simulated days. In the upper panels, the colour intensity level depends logarithmically on the tumour cell concentration.

The value of D for the homogeneous case has been estimated as the weighted average value of the diffusion coefficient for white matter, grey matter and CSF (D=0.00038cm^2/day). The concentration of tumour cells within the initial tumour has been arbitrarily assumed uniform and equal to 106 cells/mm3 [8]. Diffusion phenomena before the time point corresponding to the start of the simulation have been ignored. Regarding the parameters associated to the numerical methods used, the time step Δt, the space step size h and the convergence tolerance for the bi-conjugate gradient method have been chosen equal to 0.5 d, 0.1 cm and 10-6 respectively. The virtual tumour grows for 180 days after the initialization time point. Figure 1 shows a virtual tumor on the first and the 180th simulated day for the inhomogeneous and homogeneous scenario. Figure 2 depicts tumour cell density for the inhomogeneous case. The simulated volume appears to meet the expected clinical macroscopic behaviour of glioblastoma. Moreover, the resulting virtual tumours proved the adiabatic behaviour of the skull without artificial cell loss in the skull-brain barrier. It is noted that the threshold of tumour detection has been set equal to 8000 tumour cells/mm3 according to [5].

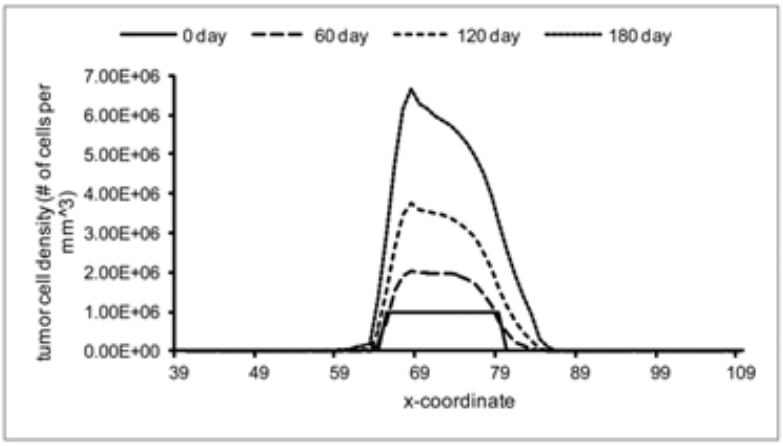

Figure 2. Tumour cell density along the x axis (the horizontal axis of the coronal plane) passing through the centre of the initial tumour for different simulated time points.

The doubling time for gliomas, which is a classical metric of glioma growth quantification, ranges from 1 week to 12 months covering the range of high to low grade gliomas [9]. Predictions of the doubling time for both cases lie within published ranges. The typical value of 2 months is observed on the 33th simulated day. Following an in silico theoretical exploration indicates that even by using a pertinent homogeneous brain based model, a rough but nonetheless informative estimate of the expected tumour doubling time can be achieved.

6. CONCLUSION

The major highlight of the paper is an explicit and thorough tri-scale numerical handling of the Neumann boundary value problem of GBM growth and invasion into the surrounding normal brain tissue in three dimensions. The heterogeneous nature of human brain and the complexity of skull geometry have been taken into consideration. Comparison of the simulation predictions with clinical observational data has supported the reliability of the model. It has also illustrated the model's potential to be used as a basis for an individualized treatment planner through in silico experimentation by exploiting the patient's multiscale data. The presented model could serve as the main component of a continuous mathematics based GBM Oncosimulator. Moreover, the study has established a generic methodology which could be translated into other mathematically similar phenomena of physics, chemistry biology and other domains.

Further model development will also include explicit tumour response to treatment and an extensive clinical adaptation and validation of the extended model.

ACKNOWLEDGEMENT

This work has been supported in part by the European Commission in the framework the projects “p-Medicine: Personalized Medicine (FP7-ICT-2009.5.3-270089)”, “CHIC: Computational Horizons in Cancer: Computational Horizons In Cancer: Developing Meta- and Hyper-Multiscale Models and Repositories for In Silico Oncology" (FP7-ICT-2011-9-600841), MyHealthAvatar (PI: 600929) and DR THERAPAT (PI: 600852). The authors would like to thank Prof. Dr med N. Graf, Director of the Pediatric Oncology and Hematology Clinic, University Hospital of Saarland, Germany and Dimitra Dionysiou PhD, ICCS, NTUA, Greece for fruitful discussions.

REFERENCES

[1] C.A. Perez, L.W. Brady, “Principles and Practice of Radiation Oncology”, Lippincott-Raven, Philadelphia, 1997.

[2] J.D. Murray, “Mathematical Biology II: Spatial Models and Biomedical Applications”, Springer-Verlag, New York, USA, 2003.

[3] G. Stamatakos, D. Dionysiou, A. Lunzer, et al. “The Technologically Integrated Oncosimulator: Combining Multiscale Cancer Modeling with Information Technology in the In Silico Oncology Context”, IEEE J. Biomed. Health Inform, 18, 2014, pp. 840-854.

[4] S. Giatili, G. Stamatakos, “A detailed numerical treatment of the boundary conditions imposed by the skull on a diffusion–reaction model of glioma tumor growth. Clinical validation aspects”, Applied Mathematics and Computation, 218, 2012, 8779-8799.

[5] K. Swanson, E. Alvord, J. Murray, “Virtual brain tumors (gliomas) enhance the reality of medical imaging and highlight inadequacies of current therapy”, Br J Cancer, 86, 2002,14 – 18.

[6] B. Bradie, "A friendly Introduction to Numerical Analysis", Pearson International, USA, 2006.

[7] S. Eikenberry, T. Sankar, M. Preul, et al., "Virtual glioblastoma: growth, migration and treatment in a three-dimensional mathematical model", Cell Prolif., 42, 2009, 511-528.

[8] G. Steel, "Basic Clinical Radiobiology", Arnold, London, UK, 2002.

[9] E. Alvord, C. Shaw, "Neoplasm affecting the nervous system in the elderly". In: Duckett S, eds. The Pathology of the Aging Human Nervous System, Lea & Febiger, Philadelphia, 1991.

THE RADIATION PROBLEM FROM A VERTICAL SHORT DIPOLE ANTENNA ABOVE FLAT AND LOSSY GROUND: VALIDATION OF NOVEL SPECTRAL DOMAIN ANALYTIC SOLUTION IN THE HIGH FREQUENCY REGIME AND COMPARISON WITH EMPIRICAL TERRAIN PROPAGATION MODELS

(selected from CEMA'16 Conference)

G. Bebrov*, S. Bourgiotis*, A. Chrysostomou*, S. Sautbekov** and P. Frangos*

* National Technical University of Athens,

9, Iroon Polytechniou Str., 157 73, Zografou, Athens, Greece

** Eurasian National University,

5, Munaitpassov Str., Astana, Kazakshtan

E-mail: pfrangos@central.ntua.gr

Abstract

A multi-channel EMG amplifier and acquisition system is proposed. The system is composed of portable signal amplifier and dedicated real-time signal processing software. The system is intended to be used with myoelectric prostheses, therefore there is an emphasis on the multichannel real-time acquisition, portability, current consumption and connectivity features. The goal of the design is to implement the latest low-power high speed technologies available on the market today and also the system is intended to test EMG signal processing algorithms. This document covers the EMG signal all the way from the muscle through the amplifier, the Driven Right Leg (DRL) noise suppressor, filtering, digitalization, PC communication, the signal processing algorithm and the real-time visualization of the results. The article includes complete schematics, analysis and tests of the device.

1. INTRODUCTION

The 'Sommerfeld radiation problem' is a well-known problem in the area of propagation of electromagnetic (EM) waves above flat and lossy ground [1]. The original Sommerfeld solution to this problem is provided in the physical space by using the 'Hertz potentials' and it does not end up with closed- form analytical solutions.

In [2], the authors considered the problem from a spectral domain perspective, which led to relatively simple 1-D integral representations for the received EM field. Then with the use of the Stationary Phase Method (SPM, [2]) novel, closed-form analytic formulas were derived, applicable in the high frequency regime.

The comparison between the analytical expressions of [2] and their integral counterparts was performed in [3] where the requirements for the applicability of the SPM method were extracted. However, as mentioned there, due to the peculiarities of the integrands, which possess particular singularities, the integral expressions of [2] are not easily evaluated using standard numerical integration techniques, as for example the adaptive Simpson's method used in [3]. As a result, a confirmation of the results by using alternative integral evaluation techniques is justified. In this work, the results for the received EM field, taken via the application of the previously mentioned SPM method are juxtaposed against the ones available in a related research work [4]. The latter are obtained via 'a claimed to be accurate' evaluation of the original Sommerfeld integrals using commercially available simulation software, namely AWAS [4].

The last part of this work is devoted to comparing the above mentioned SPM-based analytical expressions to a well–known empirical model for path loss prediction, particularly Okumura- Hata [5]. This, as well as similar comparisons to be performed in the future, will eventually determine the extent to which the easily implemented model of [2] can be used for radio wave prediction in real life scenarios.

2. PROBLEM GEOMETRY

The problem geometry is shown in Figure 1. A vertical Hertzian Dipole (HD), of dipole moment p, directed to the positive x axis, at altitude x0 above infinite, flat, lossy ground radiates time-harmonic electromagnetic (EM) waves at angular frequency $\omega=2\pi f$ ($e^{-i\omega t}$ time dependence is assumed). The relative complex permittivity of the ground is $\varepsilon_r' = \varepsilon'/\varepsilon_0 = \varepsilon_r + i\sigma/\omega\varepsilon_0$, σ being the ground conductivity, f the carrier frequency and ε_0=8,854x10-12F/m the absolute permittivity in vacuum or air. The wavenumbers of propagation are:

$$k_{01} = \omega/c_1 = \omega\sqrt{\varepsilon_1\mu_1} = \omega\sqrt{\varepsilon_0\mu_0} \tag{1}$$

$$k_{02} = \omega/c_2 = \omega\sqrt{\varepsilon_2'\mu_2} = k_{01}\sqrt{\varepsilon_r + i(\sigma/\omega\varepsilon_0)} \tag{2}$$

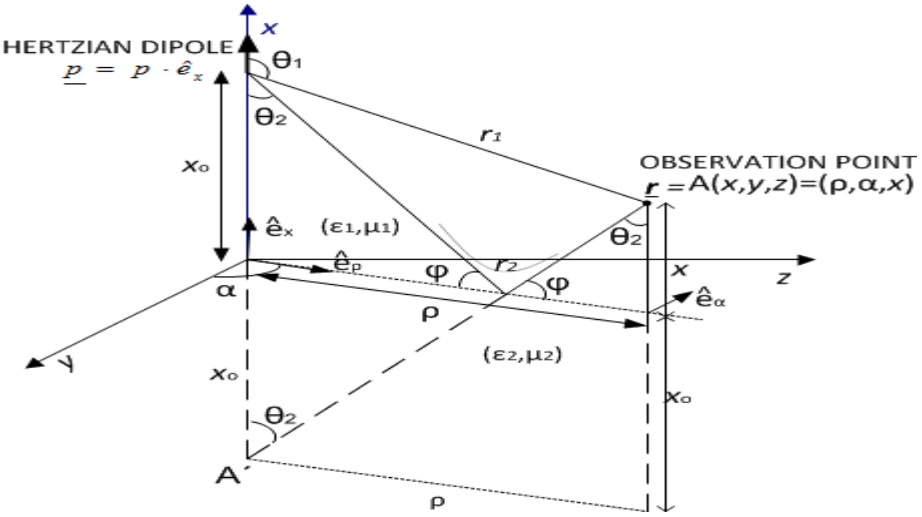

Figure 1. Geometry of the problem

In Figure 1, point A´ is the image of the HD with respect to the ground, r1 is the distance between the source and the observation point (OP), r2=(A´A) the distance between the image and the OP, θ the 'angle of incidence' at the so–called 'specular point' and φ=π/2–θ the so–called 'grazing angle'

3. INTEGRAL SPECTRAL DOMAIN REPRESENTATIONS FOR THE RECEIVED ELECTRIC FIELD AND ANALYTIC EXPRESSIONS IN THE HIGH FREQUENCY REGIME

In [2] it is shown that the electric field at the receiver's position above the ground level (x>0) can be expressed with the following integral formula (E^{LOS} denotes the direct field):

$$\underline{E}(\underline{r}) = \underline{E}^{LOS}(\underline{r}) - \frac{ip}{8\pi\varepsilon_{r_1}\varepsilon_0} \times$$

$$\times \left\{ \hat{e}_\rho \int_{-\infty}^{\infty} k_\rho^2 \frac{\varepsilon'_{r_2}\kappa_1 - \varepsilon_{r_1}\kappa_2}{\varepsilon'_{r_2}\kappa_1 + \varepsilon_{r_1}\kappa_2} e^{i\kappa_1(x+x_0)} \cdot H_0^{(1)}(k_\rho\rho) dk_\rho - \hat{e}_x \int_{-\infty}^{\infty} k_\rho^3 \frac{\varepsilon'_{r_2}\kappa_1 - \varepsilon_{r_1}\kappa_2}{\kappa_1(\varepsilon'_{r_2}\kappa_1 + \varepsilon_{r_1}\kappa_2)} e^{i\kappa_1(x+x_0)} \cdot H_0^{(1)}(k_\rho\rho) dk_\rho \right\} \quad (3)$$

where:

$$\kappa_1 = \sqrt{k_{01}^2 - k_\rho^2}\ , \quad \kappa_2 = \sqrt{k_{02}^2 - k_\rho^2} \quad (4)$$

and $H_0^{(1)}$ is the Hankel function of first kind and zero order. Application of the 'Stationary Phase Method' (SPM) to (3), leads to the following analytic expressions for the electric field vector scattered from the plane ground, in the far field region and in the high frequency regime (for x>0) [3]:

$$\underline{E}_{x>0}^{sc} = \frac{pk_{01}\cos\varphi}{4\pi\varepsilon_0\varepsilon_{r_1}(\mathrm{A'A})} \cdot \frac{\varepsilon'_{r_2}\kappa_{1s} - \varepsilon_{r_1}\kappa_{2s}}{\varepsilon'_{r_2}\kappa_{1s} + \varepsilon_{r_1}\kappa_{2s}} \cdot e^{ik_{\rho s}\rho} \cdot e^{i\kappa_{1s}(x+x_0)} \cdot (-\kappa_{1s}\hat{e}_\rho + k_{\rho s}\hat{e}_x) \tag{5}$$

where:

$$k_{\rho s} = \frac{k_{01}\,\rho}{\sqrt{(x+x_0)^2 + \rho^2}} = k_{01}\cos\varphi \tag{6}$$

$$\kappa_{1s} = \sqrt{k_{01}^2 - k_{\rho s}^2} = k_{01}\sin\varphi\,,\ \kappa_{2s} = \sqrt{k_{02}^2 - k_{\rho s}^2} \tag{7}$$

with $k_{\rho s}$ being the stationary point obtained from the SPM method [2].

4. EXPERIMENTS

In this section various illustrations are presented, comparing the model of Section 3 with (i) the accurate Sommerfeld formulation, employed in related research work [4] and (ii) Okumura – Hata empirical model for path loss prediction [5].

4.1. Comparison with Sommerfeld formulation

Figure 2 depicts the vertical component of the total received electric field, Ex, due to the radiation of a half wavelength, vertical dipole antenna above flat, lossy ground. The various plots refer to different transmitter heights. The set of the simulation parameters used for the production of these plots are shown in Table 1:

Table 1. Simulation parameters

Symbol	Description	Value
F	Operating frequency	1GHz
x_0	Height of transmitting dipole	5m, 10m, 20m, 100m, 500 m
X	Height of observation point	2m
J	Distance range	1m – 50km
P	Radiated Power[1]	150W
2h	Length of the dipole antenna	λ/2
ε_r	Relative dielectric constant of ground (typical urban ground)	4.0

Σ	ground conductivity	0.0002 S/m
[1] *Used only in the simulated scenario of Section 3. The respective value used in [4] is not mentioned*		

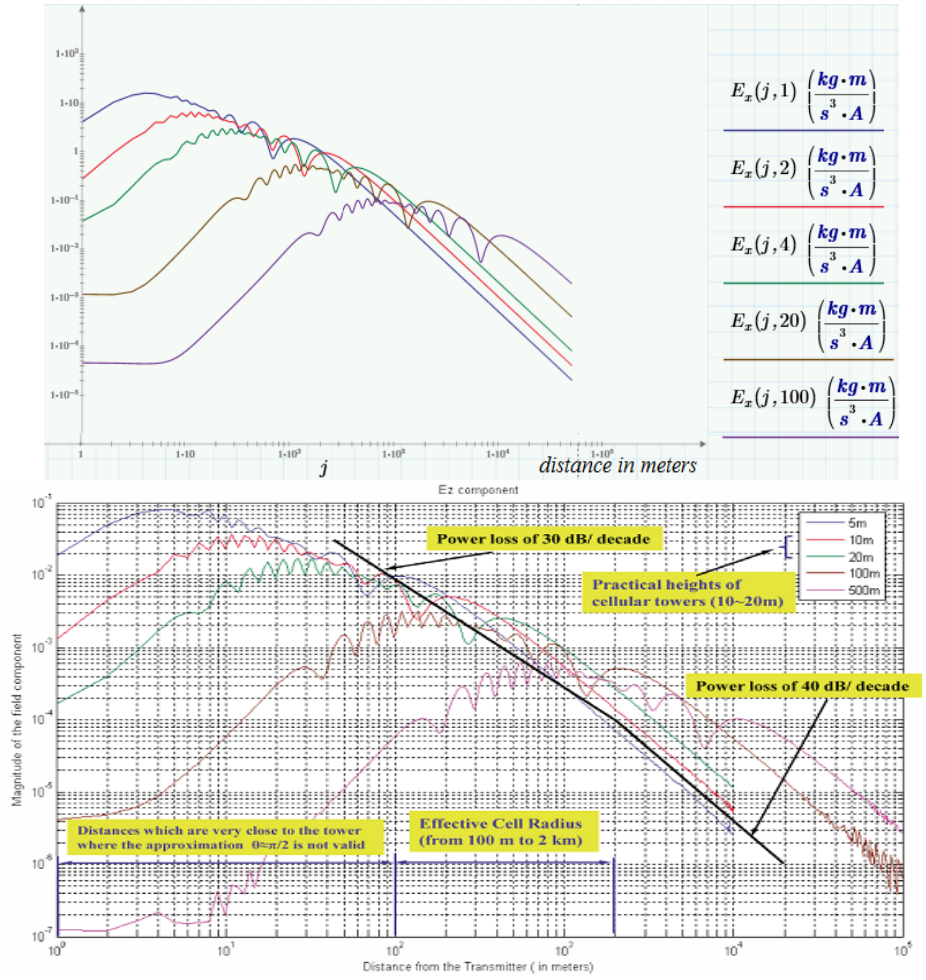

Figure 2. Variation of the magnitude of the Ex component (μV/m), for various transmitting antenna heights

The top plot of Figure 2 refers to the field values according to the analytical expressions (5) – (7), whereas the bottom one are the respective results obtained after accurately evaluating the 'Sommerfeld integrals' for the total received EM field, [4].

Evidently, the results are in very good agreement. The SPM–based analytical method of Section 3 predicts the theoretical field behavior and this is true both for the near field as well as the far field region, as they are defined in [4]. In this regard, the so-claimed in [3], 'high frequency regime analytical method' of [2], is validated for such high frequencies as 1GHz.

As another validation of the previous arguments, Figure 3 depicts the behavior of the electric field, for various scenarios regarding the electrical parameters of the ground, according to Table 2:

Table 2. Simulation parameters

Parameter	**Value**	
Operating frequency	900MHz	
Height of transmitting dipole	5m	
Height of observation point	2m	
Distance range	1m – 50km	
Radiated Power[1]	150 W	
Length of the dipole antenna	λ/2	
Ground Parameters	ε_r	σ (S/m)
Poor urban ground	4	0.001
Average ground	15	0.005
Good ground	25	0.02
Fresh water	81	0.01
Sea water	81	5.0
[1] *Used only in the simulated scenario of Section 3*		

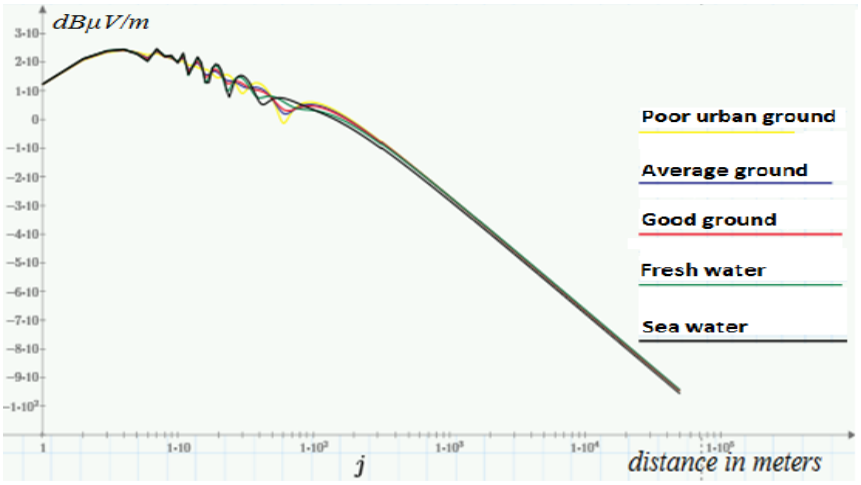

Figure 3. Variation of the magnitude of the Ex component (dBμV/m) for various types of ground

The field behavior shown in Figure 3 is almost identical to that presented in Figure 7 of [4], which is the equivalent case to the scenario considered here. In other words, the analytic expressions (5) – (7) validate the important finding of [4] (reached by numerical evaluation of the 'Sommerfeld integrals'), namely the fact that the type of the ground does not influence significantly the received EM field values.

4.2. Comparison with Okumura – Hata empirical model

A preliminary check of the model proposed hereby against the well- known Okumura – Hata (OH) empirical model [5], commonly used for predicting signal loss in land mobile radio services, is carried out. Figure 4 below illustrates the comparison.

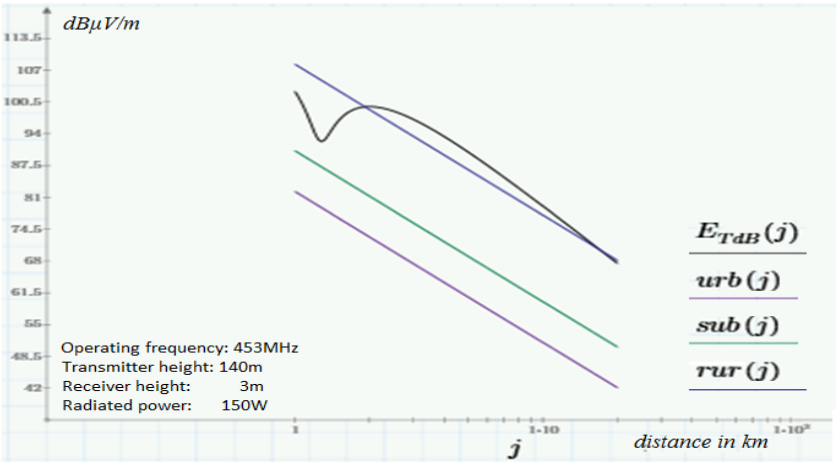

Figure 4. Comparison with OH model for urban (urb), suburban (sub) and rural (rur) environment

From Figure 4, it is evident that the proposed model exhibits similar behavior to the Okumura-Hata model for the case of an open (rural) area. On the contrary, there is an appreciable mismatch between them when applied to urban or suburban environments. A correction factor to accommodate for the specifics of the propagation environment (i.e. the presence of buildings, foliage, obstacles etc – typical to urban/suburban environment) is required and will be the subject of future research.

5. CONCLUSION – FUTURE RESEARCH

In this work, a comparison of a recently introduced solution to the 'Sommerfeld radiation problem in the spectral domain', against theoretical as well empirical approaches for the given problem is demonstrated. The proposed model leads to easily implemented analytical expressions for the received EM field and is proved to be valid in the high frequency regime.

Further validations against theoretically driven, numerical results like those of [4] used here, are required to determine the exact frequency limits of the analytic expressions (5) – (7). For this the perspective described in [3], which is believed to reduce the

precision errors appeared there, will be followed, leading to a novel spectral domain representation for the surface wave as well [note that (5) neglects the role of the surface wave].

Finally, an attempt to determine the necessary corrections that will extend the model's applicability to more complex environments is also planned. Such checks will eventually determine the adoptions necessary for turning the novel propagation model of [2] to a robust prediction tool appropriate for radio planning purposes.

REFERENCES

[1] A. N. Sommerfeld, "Propagation of Waves in Wireless Telegraphy", Ann. Phys., 28, pp. 665–736, March 1909; and 81, pp. 1135–1153, December 1926.

[2] K. Ioannidi, Ch. Christakis, S. Sautbekov, P. Frangos and S.K. Atanov, "The radiation problem from a vertical Hertzian dipole antenna above flat and lossy ground: novel formulation in the spectral domain with closed-form analytical solution in the high frequency regime", *International Journal Antennas and Propagation*, Hindawi Ed. Co., Special Issue 'Propagation of electromagnetic (EM) waves over terrain' (PEWT), vol. 2014.

[3] A. Chrysostomou, S. Bourgiotis, S.Sautbekov, K. Ioannidi and P. Frangos,"Radiation of a Vertical Dipole Antenna over Flat and Lossy Ground: Accurate Electromagnetic Field Calculation using the Spectral Domain Approach along with Redefined Integral Representations and corresponding Novel Analytical Solution", *Electronics and Electrical Engineering Journal*, Vol. 22, No. 2, 2016.

[4] T. K. Sarkar et. al., "Electromagnetic Macro Modelling of Propagation in Mobile Wireless Communication: Theory and Experiment", *IEEE Antennas and Propagation Magazine*, Vol. 54, No. 6, pp. 17–43, Dec. 2012.

[5] Hata, Masaharu, "Empirical formula for propagation loss in land mobile radio services," IEEE Transactions on Vehicular Technology, Vol.VT-29, No.3, pp.317 – 325, August 1980.